Newton-Raphson solver for finite element methods featuring nonlinear hysteresis models (repository copy)

Article:

Chama, A., Gerber, S., Wang, R-J., (2018) Newton-Raphson solver for finite element methods featuring nonlinear hysteresis models, *IEEE Transactions on Magnetics*, 54(1): 7400108, January 2018; ISSN: 1941-0069

http://dx.doi.org/10.1109/TMAG.2017.2761319

Newton-Raphson Solver for Finite Element Methods Featuring Nonlinear Hysteresis Models

Abdoulkadri Chama, Stiaan Gerber, *Member,* Rong-Jie Wang, *Senior Member, IEEE*

Abstract – It is well known that the Newton-Raphson method is the most popular iterative method for nonlinear finite element problems. The method has a quadratic convergence. Under certain conditions on the Jacobian of the functional and the initial guess the Newton-Raphson method can converge very fast. However, standard evaluation of such Jacobian may not be possible for the solution of nonlinear hysteresis field problems. This is due to the nature of the magnetization curves that may not be differentiable or possess a very steep gradient. In this paper an alternative finite element implementation using Newton-Raphson method for hysteresis field problems is described in detail. To improve the convergence of the method, a method for evaluation of the initial guess is also proposed. It is shown that the Newton method can be reliably used for solving hysteresis field problems.

***Index Terms*—Finite element, Newton-Raphson method, Hysteresis-curve, and weak derivatives**

I. Introduction

Finite element implementation in the context of electromagnetism often lead to the resolution of nonlinear problems. The most popular iterative method, the *Newton-Raphson method*, does not perform well when dealing with materials exhibiting hysteresis. As a remedy, alternative algorithms have been proposed. Among them is the fixed point method [1]–[3], where a uniform contraction of the functional has to be satisfied in order to improve the speed of convergence, though the method is known to be very slow in general with first order convergence. The contraction condition is obtained by the computation of a fictitious permeability and magnetization vector in the nonlinear ferromagnetic material region.

Methods free of derivation are the extensions of the successive over-relaxation (SOR) method, which are considered as competitors to the Newton iteration. However, the published studies are either theoretical with no experimental validation [4] or with a very limited number of equations [5]. Higher order than Newton method have been developed for nonlinear problems in [6]–[8] and reference therein. These methods are based on a higher evaluation or derivation of the functional than the Newton method. Therefore, when dealing with large system of equations such as in finite element analysis, this can make the program very slow or at least cumbersome and unattractive [9], [10]. Extensive details for theoretical analysis of the solution of nonlinear equations can be found in [9], where the authors stressed the significance of experimental validation of the performance of iterative solvers. For this reason it is reasonable to maintain popular algorithm such as the Newton iteration for problems that have extensive use in practice.

The objective of this work is to show the possibility of the implementation of the Newton method in the context of the hysteresis field problems. First, it is well known that one of the drawbacks of the Newton method is related to the evaluation of the Jacobian [1], which may not always exist. Such Jacobian in the case of vector-field formulation involves taking the derivative of some non-smooth interpolation data. Instead of imposing the strong differentiability of the curve we make use of weak differentiability. This approach seems more appropriate since the finite element is by essence considered only in the sense of distribution.

The rest of the paper is structured as follows: In Section II, the derivation of the governing problem is discussed. In Section III its linearized form, for the need of Newton implementation, is presented. In Section IV the evaluation of such Jacobian and the choice of the initial guess for rapid convergence of the method are discussed. Section V will be devoted to numerical tests and comparison. Conclusions are given in Section VI.

II. Finite element formulations

In this section, the governing equations describing the behavior of nonlinear ferromagnetic materials such as electrical steels is briefly reviewed.

Firstly, the magnetic flux density is defined as

$$\boldsymbol{B} \equiv \mu_0(\boldsymbol{H} + \boldsymbol{M}) = \nabla \times \boldsymbol{A} \tag{1}$$

where $\boldsymbol{H}$ is the magnetic field strength and $\boldsymbol{M}$ is the magnetization density or magnetization [11]. Generally, $\boldsymbol{B}$, $\boldsymbol{H}$ and $\boldsymbol{M}$ are vector fields. By expressing $\boldsymbol{B}$ as the *curl* of the magnetic vector potential $\boldsymbol{A}$, the Coulomb Gauge condition ($\nabla \cdot \boldsymbol{A} = 0$) is ensured and the problem is reduced to solving Ampère's law:

$$\nabla \times \boldsymbol{H} = \boldsymbol{J} \tag{2}$$

Here, we consider the static case for simplicity, but the theory is just as applicable to transient formulations.

In (1), the magnetization $\boldsymbol{M}$ is generally a function of $\boldsymbol{H}$. In many materials, the magnetization is linearly dependent on $\boldsymbol{H}$ over a region of interest, such that [11]

$$\boldsymbol{M} = \chi_m \boldsymbol{H} \tag{3}$$

This work was supported in part by Subcommittee B Post-Doctoral Fellowship, Stellenbosch University, and in part by a National Research Foundation IFRR grant, all of South Africa.

The authors are with the Department of Electrical and Electronic Engineering, Stellenbosch University, Private Bag X1, Matieland 7602, South Africa (e-mails: chama@aims.ac.za; sgerber@sun.ac.za; rwang@sun.ac.za)

Manuscript received xx xx, 2017; revised xx xx, 2017.

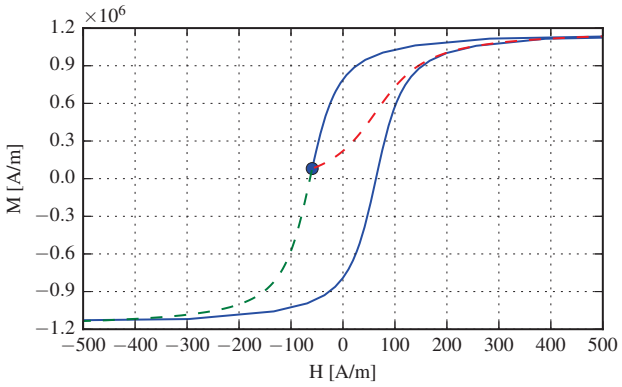

Fig. 1. Hysteresis model showing history (solid line) and possible future trajectories in the forward (low dashed lined) and reverse (top dashed line) directions.

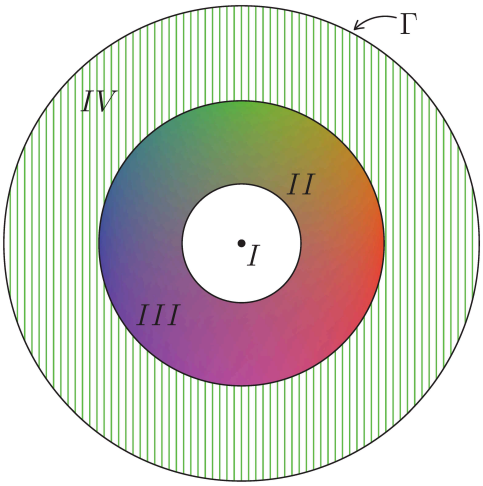

Fig. 2. Domain Ω containing regions $I-V$ characterized by their permeability

In such materials, it is especially convenient to define the permeability of the material as

$$\mu \equiv \mu_0(1+\chi_m) \tag{4}$$

Using the permeability, $\boldsymbol{M}$ can be eliminated and the flux density can be expressed as

$$\boldsymbol{B} = \mu \boldsymbol{H} \implies \boldsymbol{H} = \frac{1}{\mu}\nabla \times \boldsymbol{A} \tag{5}$$

This leads to the following, well known, governing equation:

$$\nabla \times \frac{1}{\mu}\nabla \times \boldsymbol{A} = \boldsymbol{J} \tag{6}$$

Modeling materials with nonlinear BH characteristics can be accomplished in one of two ways. The most common approach is to use (6), where μ is a nonlinear (possibly tensor) function of $\boldsymbol{B}$. This approach is very effective when the material can be characterized by a simple single-valued BH-curve. However, in other circumstances, (6) may not be the most appropriate formulation to use. In this paper, the focus falls on modeling nonlinear materials exhibiting hysteresis. The hysteresis model presented in [12] is considered. The scalar version of the model can be described by the following equation:

$$H(M) = H^{\text{qm}}(M) + H^{\text{anh}}(M) \tag{7}$$

where the total H field is calculated as the sum of a hysteretic component, $H^{\text{qm}}(M)$ and an anhysteric component, $H^{\text{anh}}(M)$. For details of the implementation, readers are referred to the literature. The model keeps track of the state (history) of the material and provides possible future trajectories. A typical state of such a model is shown in Fig. 1. In effect, this model provides $\boldsymbol{H}$ as a function of $\boldsymbol{M}$ and thus, an alternative finite element formulation is used where μ is not introduced and $\boldsymbol{M}$ remains.

Solving (1) for $\boldsymbol{H}$, one obtains

$$\boldsymbol{H} = \frac{1}{\mu_0}\nabla \times \boldsymbol{A} - \boldsymbol{M} \tag{8}$$

and when (8) is substituted into (2), we obtain

$$\nabla \times \frac{1}{\mu_0}\nabla \times \boldsymbol{A} = \boldsymbol{J} + \nabla \times \boldsymbol{M} \tag{9}$$

where $\boldsymbol{M}$ is a nonlinear function of $\boldsymbol{H}$. Note that, although (9) takes the form of the governing equation often used to model permanent magnet regions, here it is used in a different manner to model nonlinear materials with hysteretic behavior.

Permanent magnets are modeled using the following characteristic equation:

$$\boldsymbol{B} = \mu_m \boldsymbol{H} + \boldsymbol{B_r} \tag{10}$$

where μ_m is the magnet's recoil permeability and $\boldsymbol{B_r}$ is the remanent flux density. Thus, in permanent magnet regions, the following governing equation may apply:

$$\nabla \times \frac{1}{\mu_m}\nabla \times \boldsymbol{A} = \boldsymbol{J} + \nabla \times \frac{\boldsymbol{B_r}}{\mu_m} \tag{11}$$

where μ_m and $\boldsymbol{B_r}$ are constants.

III. Problem Formulation and its Linearized Form

For application let's consider a generic magneto-static problem occupying a bounded region $\Omega \subset \mathbb{R}^2$, with Lipschitz boundary Γ, as depicted in Fig. 2. The numeration define the regions characterized by their respective permeability. Γ is the frontier of Ω where Dirichlet boundary condition ($\boldsymbol{A} = \boldsymbol{0}$) is imposed.

A. The governing equation

Using the properties of the *curl* operator on the left hand side of (9) and (11) we obtain:

$$-\frac{1}{\mu_0}\nabla^2 A = J + \frac{\partial M_y}{\partial x} - \frac{\partial M_x}{\partial y} \tag{12}$$

in the nonlinear material and air-gap regions, and

$$-\frac{1}{\mu_m}\nabla^2 A = J + \frac{\partial M_y}{\partial x} - \frac{\partial M_x}{\partial y} \tag{13}$$

in the permanent magnet regions, where $\boldsymbol{M} = \boldsymbol{Br}/\mu_m$ in (13).

Since our interest is to handle the nonlinearity, (12) and (6) will be the governing equations for the problem, where the nonlinearity of the material in the above formulation is carried

by the magnetization vector $\boldsymbol{M}$. Instead of using BH data we use MH data provided from the positive feedback theory in [13] to update the values of $\boldsymbol{M}$. An example of such MH data is given by the dashed curves in Fig. 1.

B. Finite element implementation

The variable $\boldsymbol{A}$ will be defined in the Sobolev spaces $H^m(\Omega)$, for non-negative integer m and associated with inner product and norm, such that for given u and v in $H^m(\Omega)$ we have:

$$(u,v)_m := \int_\Omega \sum_{|\alpha|\le m} D^\alpha u(x) v(x) \mathrm{d}x \quad \text{and} \quad \|v\|_m := (v,v)_m^{1/2}$$

where $\alpha = (\alpha_1, \cdots, \alpha_n)$, $n \le m$, α_i are positive integers and for some function f that is $m-$times differentiable

$$D^\alpha f = \frac{\partial^{|\alpha|} f}{\partial \alpha_1 \cdots \partial \alpha_n}\,.$$

Using integration by parts the problem takes the following weak formulation (III-B):

$$-\frac{1}{\mu_0}(\nabla A, \nabla v)_0 = (J,v) + \left(\frac{\partial M_y}{\partial x} - \frac{\partial M_x}{\partial y}, v\right) \qquad (14)$$
$$\forall\, v \in H_0^1(\Omega)$$

where $H_0^1(\Omega) = \{v \in H^1(\Omega)\,|\, v = 0, \ \text{ in } \partial\Omega\}$.

If we consider N_i, (where $i = 1, \cdots, N$) to be the finite element shape functions, the discrete weak formulation of (III-B) is the problem of finding $A_h = \sum_{i=1}^{N} A_i N_i$ such that

$$\frac{1}{\mu_0}(\nabla A_h, \nabla N_i)_0 = (J,v) + (\frac{\partial M_y}{\partial x} - \frac{\partial M_x}{\partial y}, N_i)_0 \qquad (15)$$
$$\text{for } i = 1, \cdots, N.$$

Note that in (III-B) and (15) the magnetization vector $\boldsymbol{M}$ vanishes in the air-gap regions. Now consider the mapping:

$$\begin{aligned} \boldsymbol{\mathcal{F}} :& \mathbb{R}^N \to \mathbb{R}^N \\ & \boldsymbol{v} \mapsto \frac{1}{\mu}\boldsymbol{K}\boldsymbol{v} - \boldsymbol{b}(\boldsymbol{M}(\boldsymbol{v}))\,, \end{aligned}$$

where μ is the permeability of the medium, assembling the right and left hand side of (15) we obtain the system of algebraic equations:

$$\boldsymbol{\mathcal{F}}(\boldsymbol{A}) = \frac{1}{\mu_0}\boldsymbol{K}\boldsymbol{A} - \boldsymbol{b}(\boldsymbol{M}(\boldsymbol{A})) = \boldsymbol{0}\,. \qquad (16)$$

The matrice $\boldsymbol{K}$ and vector $\boldsymbol{b}$ in (16) are the finite element assembly of the left and right hand side of (15), respectively.

The problem (16) above does not involve nonlinear variation of the permeability, but the vector $\boldsymbol{b}$ is nonlinear in $\boldsymbol{A}$. For the fixed point method, as introduced in [1]–[3], [14], (16) can be reinterpreted as

$$\boldsymbol{\mathcal{F}}(\boldsymbol{A}) = \frac{1}{\mu_{\text{FP}}}\boldsymbol{K}\boldsymbol{A} - \boldsymbol{b}(\boldsymbol{M}_{\text{FP}}) = \boldsymbol{0}\,, \qquad (17)$$

where μ_{FP} and $\boldsymbol{M}_{\text{FP}}$ are being approximated during the computational process to insure rapid convergence of the method.

The application of the Newton method to the nonlinear problems (16) and (17) results in the following linearized problem: given the vector potential $\boldsymbol{A}_k$ find $\delta\boldsymbol{A}_k = \boldsymbol{A}_{k+1} - \boldsymbol{A}_k$ and hence $\boldsymbol{A}_{k+1} = \delta\boldsymbol{A}_k + \boldsymbol{A}_k$ such that:

$$\boldsymbol{\mathcal{J}\mathcal{F}}(\boldsymbol{A}_k) \times \delta\boldsymbol{A}_k = -\boldsymbol{\mathcal{F}}(\boldsymbol{A}_k)\,. \qquad (18)$$

where $\boldsymbol{\mathcal{J}\mathcal{F}}$ is the Jacobian of the functional $\boldsymbol{\mathcal{F}}$.

IV. Jacobian and Initial Guess

The resolution of the nonlinear system (18) requires a starting point, $\boldsymbol{A}_0$, and the evaluation of the Jacobian $\boldsymbol{\mathcal{J}\mathcal{F}}(\boldsymbol{A}_k)$ at each k^{th} iteration. In this section we discuss how to define $\boldsymbol{A}_0$ for faster convergence of the Newton method and how to evaluate the Jacobian regardless of the smoothness of the data.

A. Choice of the initial guess

The Newton method hardly converges if the initial guess is not chosen properly [15]. To construct a good approximation of the initial guess we use the idea where the analytical solution to problem (18) has been provided with constant values of the permeability in the nonlinear ferromagnetic material. Therefore, the initial guesses of (16) can be defined by solving the linear problem:

$$\frac{1}{\mu_0}\boldsymbol{K}\boldsymbol{A}_0 = \boldsymbol{b} \qquad (19)$$

where $\boldsymbol{A}_0$ satisfies the Dirichlet boundary conditions $\boldsymbol{A}_0 = \boldsymbol{0}$ on $\partial\Omega$. To show the closeness of the initial guess to the exact solution we have considered the vector potential in the back yoke, just above the slots of the machine shown in Fig. 8b. The nonlinear solution has been compared to linear solutions with varying values of the permeability. It can be seen that high values of the permeability produce good approximations to the exact solution. All the linear solutions for the vector potential shown in Fig. 3 are good candidates for the initial guess compared to a trivial or random initial guess. Using the equivalence between the MH and BH formulations, we make the assumption that a good initial guess for the MH formulation can also be obtained by a linear solution of (19).

B. Evaluation of the Jacobian

To implement the Newton-Raphson method the main challenge when dealing with the hysteresis curve is the evaluation of its Jacobian at critical points (e.g. Fig. 4). In this section we present an approach for computing the Jacobian $\boldsymbol{\mathcal{J}\mathcal{F}}(\boldsymbol{A}_k)$ regardless of the smoothness of the MH-data.

For problem (16) the Jacobian can be expressed as:

$$\boldsymbol{\mathcal{J}\mathcal{F}}(\boldsymbol{A}) = \frac{1}{\mu_0}\boldsymbol{K} - \boldsymbol{\mathcal{J}b}(\boldsymbol{M}), \qquad (20)$$

where $\boldsymbol{\mathcal{J}b}(\boldsymbol{M}) = \dfrac{\partial \boldsymbol{b}(\boldsymbol{M})}{(\partial A_1, \cdots, \partial A_N)}$. To compute the components of $\boldsymbol{\mathcal{J}b}(\boldsymbol{M})$ on an element T of the mesh it is necessary to find the value m of the magnetization vector $\boldsymbol{M}$ such that:

$$H_k(m_k) + m_k = \frac{1}{\mu_0}B_k^e \qquad (21)$$

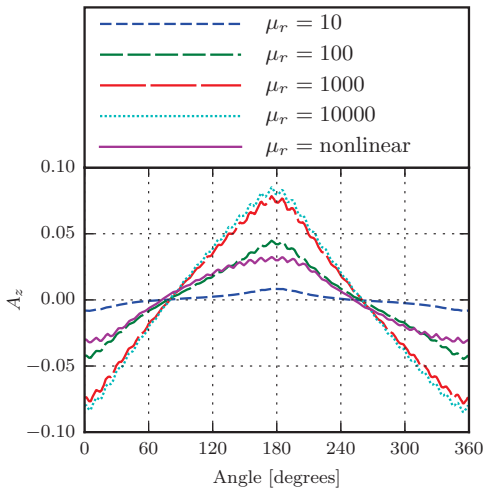

Fig. 3. Vector potential in the back yoke of the machine in Fig. 8b.

where B_k^e is the flux density at the corresponding element and $H_k(m_k)$ the magnetic field intensity at m_k. The k subscripts denote either the x or y-components.

Problem (21) is nonlinear in m and needs to be solved at each iteration for each element. To make the resolution much faster and easier one can first introduce the set of data, $F_k = H_k + M_k$. Using the interpolation of F_k the solution of (21) can be found as the intersection of F_k and the line $y = \frac{1}{\mu_0} B_k$ as shown in Fig. 5. It can also be observed from Fig. 5 that the interval $[m_i, m_{i+1}]$ contains the root $m^\star$ of problem (21), which is the smallest distance from points of $F_k - \frac{1}{\mu_0} B_k$ to the x-axis. Instead of globally interpolating the data F_k, which is computationally costly, one can interpolate the data around m_i and m_{i+1} to find a good approximation of $m^\star$; for a cubic interpolation the set of data $\{m_{i-1}, m_i, m_{i+1}, m_{i+2}\}$ or $\{m_i, m_{i+1}, m_{i+2}, m_{i+3}\}$ can be interpolated.

The Jacobian of $\boldsymbol{b}(\boldsymbol{M})$ depends only on the derivative of M with respect to the nodal values of A. Assuming the MH-curve to be strongly differentiable, the derivatives with respect to A_i of the left and right hand side of (21) give:

$$\left(\frac{\partial H_k(m_k)}{\partial m_k} + 1\right) \frac{\partial m_k}{\partial A_i} = \frac{1}{\mu_0} \left(\frac{\partial B_k^e}{\partial A_i}\right) \tag{22}$$

Then (22) implies that

$$\frac{\partial m_k}{\partial A_i} = \left[\mu_0 \left(\frac{\partial H_k(m_k)}{\partial m_k} + 1\right)\right]^{-1} \left(\frac{\partial B_k^e}{\partial A_i}\right) \tag{23}$$

Note that H varies always in the direction of M, which implies that $\frac{\partial H(m_k)}{\partial m_k} + 1 \neq 0$. Therefore, the expression (23) is well defined.

However, at certain critical points (e.g. Fig. 5) such as at angular, inflection or discontinuity points the equality in (22) ceases to be satisfied as the derivative $\frac{\partial H(m_k)}{\partial m_k}$ is undefined.

Since the finite element method is in essence based on weak formulations, it makes more sense to deal with distributional derivatives. Indeed, the linear shape functions are in general not differentiable and their Laplacian $\nabla^2 N_i$ are evaluated via weak differentiability. A graphical interpretation of N_i and

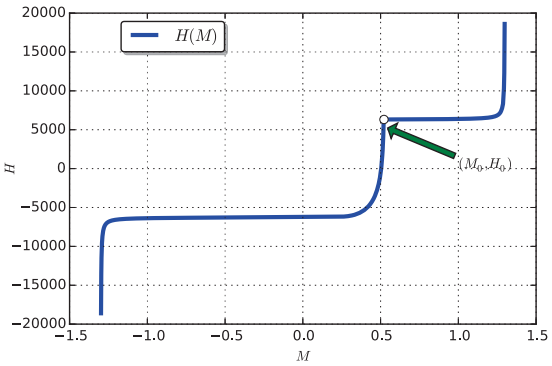

Fig. 4. Critical point of the Hysteresis curve.

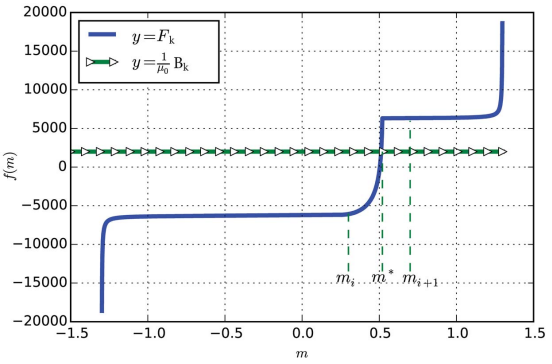

Fig. 5. Graphical interpretation of $m^\star$ solution to (21).

their derivatives in a patch K_i are depicted in Figs. 6 and 7. Fig. 7 is a projection of a 3D graph in a 2D plane, a closer look at the vertical axis shows different values, indicated in dot, of the derivative at point (x_i, y_i).

To evaluate $\frac{\partial m_k}{\partial A_i}$ a weak form of (21) can be constructed as follows:

$$(f(m_k), \varphi)_0 = \frac{1}{\mu_0} (B_k, \varphi)_0 \tag{24}$$

where φ is an interpolation test function and $f(m_k) = H(m_k) + m_k$ is the interpolation of $\boldsymbol{F}$. It then follows that

$$\left(\frac{\partial f(m_k)}{\partial A_i}, \varphi\right)_0 = \frac{1}{\mu_0} \left(\frac{\partial B_k}{\partial A_i}, \varphi\right)_0 \tag{25}$$

$$\left(\frac{\partial f(m_k)}{\partial m_k} \frac{\partial m_k}{\partial A_i}, \varphi\right)_0 = \frac{1}{\mu_0} \left(\frac{\partial B_k}{\partial A_i}, \varphi\right)_0 \tag{26}$$

The derivatives in (25) and (26) are evaluated at $m_k = m_k^\star$, therefore, $\frac{\partial m_k}{\partial A_i}$ is fixed term.

From (26) we can write:

$$\frac{\partial m_k}{\partial A_i} = \frac{1}{\mu_0 \left(\frac{\partial f(m_k)}{\partial m_k}, \varphi\right)_0} \left(\frac{\partial B_k}{\partial A_i}, \varphi\right)_0 \tag{27}$$

Using integration by part and the weak differentiability of $f(m_k)$ at $m_k = m_k^\star$ the denominator in (27) can be expressed as:

$$\left(\frac{\partial f(m_k)}{\partial m_k}, \varphi\right)_0 = -\mu_0 \left(f(m_k), \frac{\partial \varphi}{\partial m_k}\right)_0 \tag{28}$$

Equations (20) to (26) are the components of the vectorized formulation of $\boldsymbol{M}$ and $\boldsymbol{H}$. Two dimensional vectorized form of

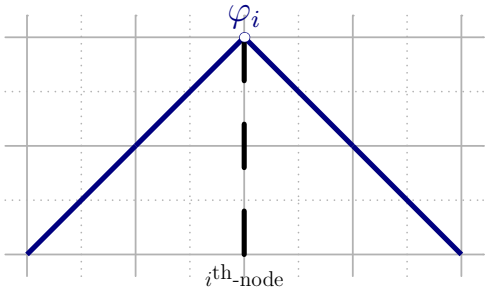

(a) One dimensional shape function defined on a compact support.

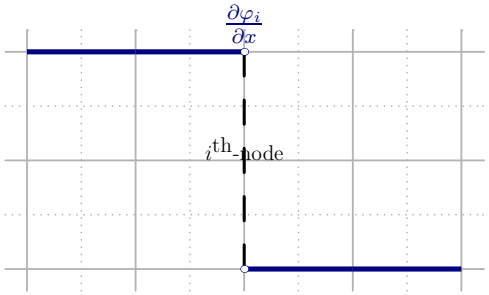

(b) Derivative of φ_i at the i^{th}-node in its compact support.

Fig. 6. Finite element shape function and their derivatives

the hysteresis data are obtained by using the one dimensional data depicted in Fig. 4 and 5 and the vectorial transformation can be realized by using the method described in [14], where given the magnetic field strength $H_\varphi(\boldsymbol{B}(\varphi))$ the transformation formula read as:

$$\boldsymbol{H}(\boldsymbol{B}) = \frac{1}{Q(N)} \sum_{i=1}^{N} \boldsymbol{e}_\varphi H_\varphi(B_\varphi)\,, \tag{29}$$

where N is the number of projection vectors $\boldsymbol{e}_\varphi$, Q an identification number. Clear description of these parameters and the projection B_φ of the magnetic field is given in [14]. The field strength $\boldsymbol{H}_\varphi$ is derived from the scalar model of Fig. 4. To obtain $H_\varphi(B_\varphi)$ we use the scalar relation $B = \mu_0 \left(H(B_\varphi) + M(B_\varphi)\right)$ and the graph 4 to solve for $M(B_\varphi)$.

To explicitly formulate the Jacobian one may observe first that the first term of the system (16) is linear and hence its Jacobian will produce $\frac{1}{\mu_0}\boldsymbol{K}$. For the second term which is nonlinear its entries are defined by $\frac{\partial \boldsymbol{b}_i(\boldsymbol{M})}{\partial A_j}$ where $\boldsymbol{b}_i(\boldsymbol{M})$ is the i^{th} element of $\boldsymbol{b}(\boldsymbol{M})$. Considering the components of $\boldsymbol{M}^e$, on an element, to be m_1 and m_2 we have

$$\boldsymbol{b}_i(\boldsymbol{M}) = (\nabla \times \boldsymbol{M}^e, N_i) = \left(m_2, \frac{\partial N_i}{\partial x}\right) - \left(m_1, \frac{\partial N_i}{\partial y}\right)\,,$$

which can then be used to obtain

$$\frac{\partial \boldsymbol{b}_i(\boldsymbol{M})}{\partial A_j} = \left(\frac{\partial m_2}{A_j}, \frac{\partial N_i}{\partial x}\right) - \left(\frac{\partial m_1}{A_j}, \frac{\partial N_i}{\partial y}\right)\,.$$

Note that the entries of the Jacobian are evaluated at the element level which can then be used to assemble the global matrix.

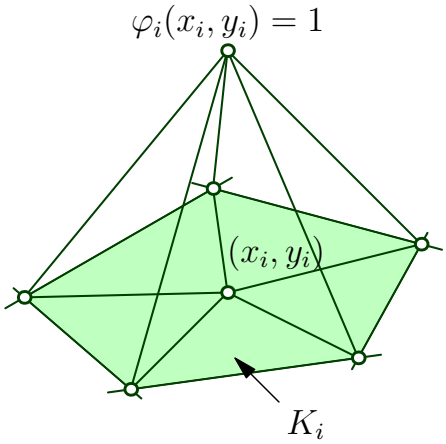

(a) Two-dimension shape function in a compact support K_i.

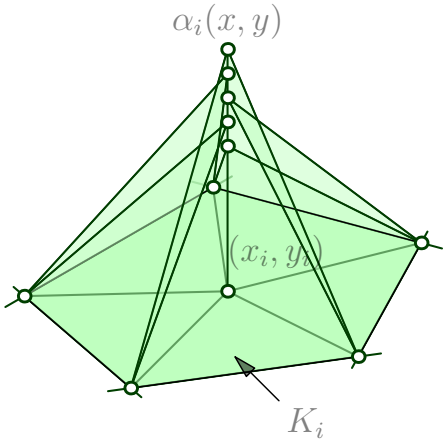

(b) α_i is the derivatives of φ_i at the i^{th}-node in K_i.

Fig. 7. Finite element shape functions and their derivatives, [17].

V. Numerical Validation of the Theory

This section is devoted to the numerical validation of the theory discussed in Section II. Two examples have been considered, see Figs. 8a and 8b, to demonstrate the reliability of the Newton method in the context of hysteresis field problems. The convergence performance of the proposed method under particular choice of the initial guess is also evaluated.

Both the conventional (BH data based) and the proposed finite element formulations (MH data based) are implemented for both examples. The BH curve used in the simulations is shown in Fig. 9. Flowcharts describing the implementation of both methods are given in Figs. 10 and 11.

The magnetic flux distribution obtained from the finite element simulations for both examples is shown in Fig. 12.

The accuracy of the method is evaluated by comparing the solutions obtained from the MH formulation and the BH formulation. The relative errors as illustrated in Figs. 13(a) and 13(b) clearly show the very close agreement between the two implementations.

To prove the effect of choosing the initial guess the absolute errors, $\boldsymbol{A}^{k+1} - \boldsymbol{A}^k$, and the time of convergence by the different formulations are given in Tables I-IV. The initial guesses

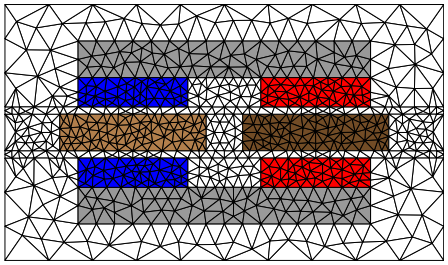

(a) Linear PM machine example.

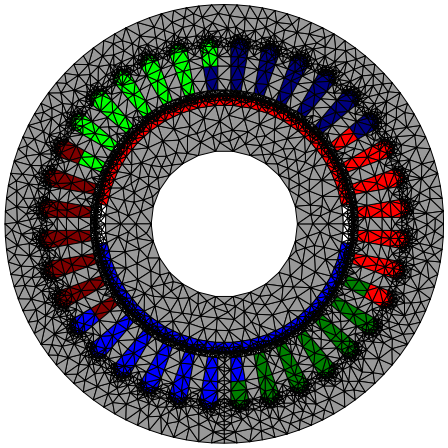

(b) Rotary PM machine example.

Fig. 8. Machine examples used for numerical validation of the proposed method.

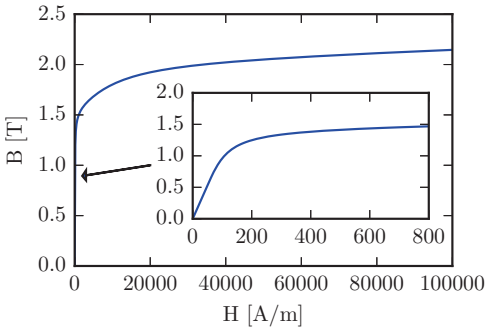

Fig. 9. Nonlinear BH-curve used for numerical validation.

are chosen in both cases by solving the linear problem with different permeabilities for the BH formulation and different values of the magnetic field strength m_0, respectively. For completeness particular choices of initial guess such as $\boldsymbol{A}$ to be trivial and randomly generated $\boldsymbol{A}$ are also considered.

It is clear from the above that the initial guesses derived

TABLE I
BH FORMULATION: EXAMPLE 1, FIG. 12A

μ_r	Error	Time in seconds
10	3.29×10^{-12}	3.02
10^3	7.50×10^{-14}	4.75
10^7	7.63×10^{-14}	3.05
$\boldsymbol{A} = \mathbf{0}$	7.63×10^{-6}	9.16
10^{-10}:	no convergence found	

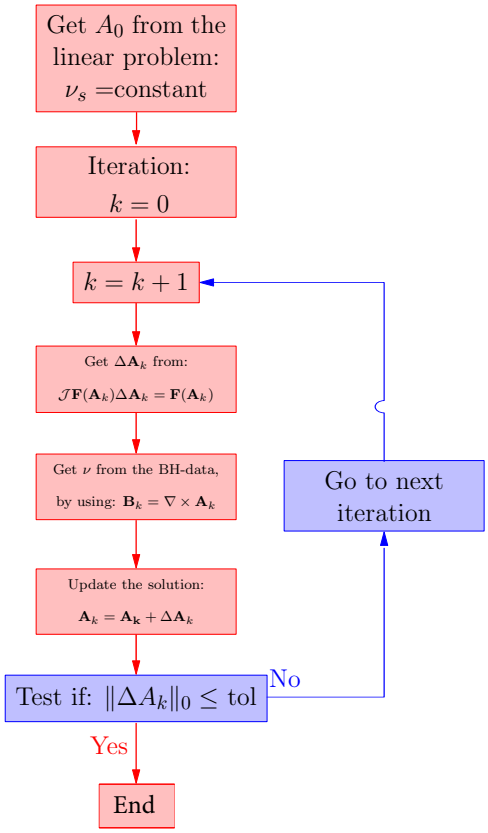

Fig. 10. BH implementation.

TABLE II
MH FORMULATION: EXAMPLE 1, FIG. 12A

m_0	Error	Time in seconds
0	1.07×10^{-14}	2.66
5×10^3	1.88×10^{-9}	0.77
10^7	4.79×10^{-14}	3.15
10^{-7}	1.88×10^{-11}	9.82
$\boldsymbol{A} = 0$:	no convergence found	

TABLE III
BH FORMULATION: EXAMPLE 2, FIG. 12B

μ_r	Error	Time in seconds
10^3	4.67×10^{-14}	3.97
10^{-10}	7.92×10^{-5}	24.92
10^7	5.00×10^{-14}	12.18
$\boldsymbol{A}$ = random:	no convergence found	

TABLE IV
MH FORMULATION: EXAMPLE 2, FIG. 12B

m_0	Error	Time in seconds
0	1.48×10^{-12}	5.96
5×10^3	1.48×10^{-14}	1.48
10^7	4.93×10^{-11}	7.15
$\boldsymbol{A}$ = random:	no convergence found	

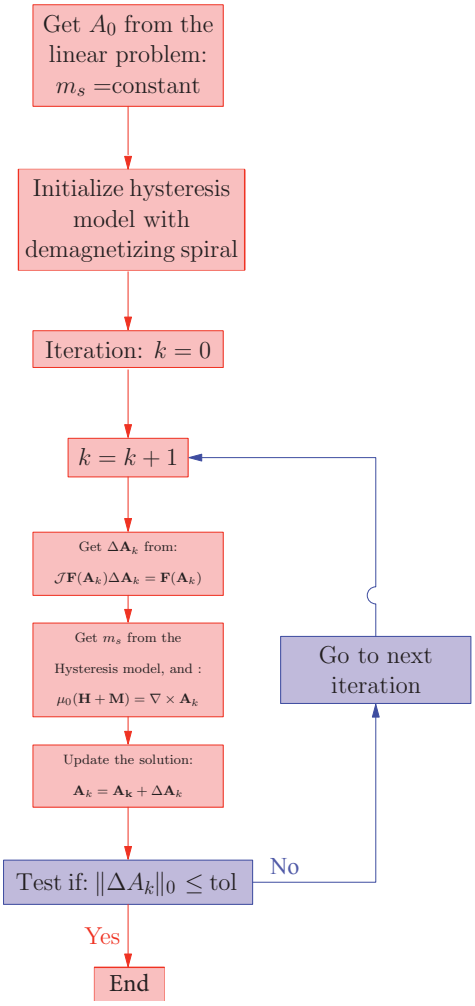

Fig. 11. MH implementation. Here m_s is a constant value of the magnetization vector $\boldsymbol{M}$.

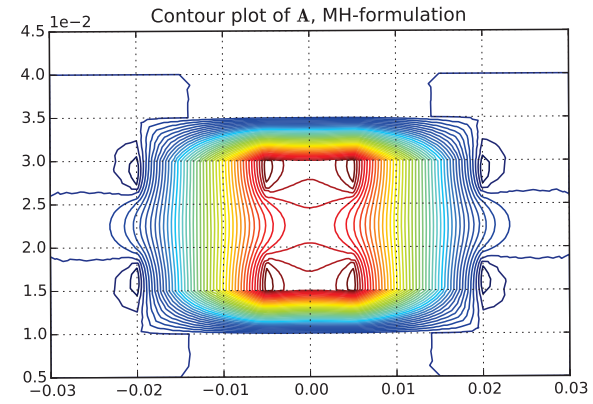

(a) Example of a linear machine.

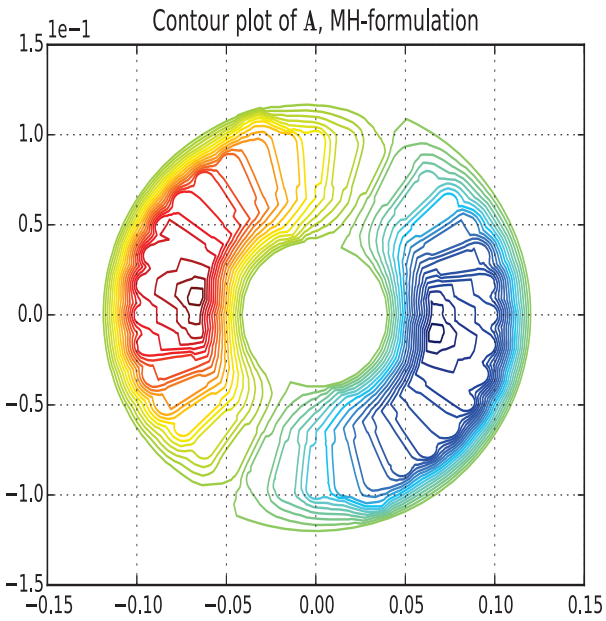

(b) Example of a rotating machine.

Fig. 12. Contour plots of vector potential $\boldsymbol{A}$

by solving linear formulations with appropriate choice of μ_r in the case of BH and m_0 in the case of MH improve dramatically the speed of convergences.

To also ensure that the MH formulation does respond to the Newton iteration convergence criteria, the residual of such convergence against the number of iterations is also plotted in Fig. 14. Comparable convergence performances are evident.

VI. Conclusion

The Newton-Raphson method is a commonly used iterative method for nonlinear problems. The method has a quadratic convergence. Under certain conditions on the Jacobian of the functional and the initial guess the Newton-Raphson method converges very fast. However, standard evaluation of such Jacobian may not be possible for the solution of nonlinear hysteresis field problems. This is due to the nature of the MH and sometimes BH curves that may not be differentiable or possess a very steep gradient. To the best knowledge of the authors, there has not been published work that considers using Newton method for the hysteresis field problem. In this paper an alternative finite element implementation using Newton-Raphson method for hysteresis field problems has been proposed and described in detail. The weak differentiability of the proposed approach makes the evaluation of Jacobian possible regardless of the structure of the hysteresis models. To improve the convergence of the method, a method for evaluation of the initial guess is also proposed. For validation purpose, both the proposed formulation and the standard BH formulation are implemented in two case studies. The results from both methods show close agreement. It has shown that the Newton method can be reliably used for solving hysteresis field problems.

References

[1] E. Dlala and A. Arkkio. Analysis of the convergence of the fixed-point method used for solving nonlinear rotational magnetic field problems, *IEEE Trans on Magnetics*, Vol. 44, No. 4, April 2008.

[2] E. Dlala, A. Belahcen, and A. Arkkio. Locally convergent fixed-point method for solving time-stepping nonlinear field problems, *IEEE Trans on Magnetics*, Vol. 43, No. 11, April 2007.

[3] G. Meunier (Editor). The Finite element method for electromagnetic modeling, 177–244, Wiley-ISTE, 2008.

[4] W. Zhang. Methods for solving nonlinear systems of equations, University of Washington, August 12 2013.

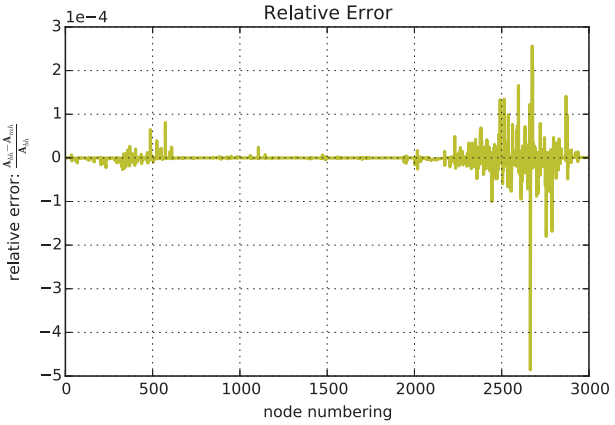

(a) Example of a linear machine.

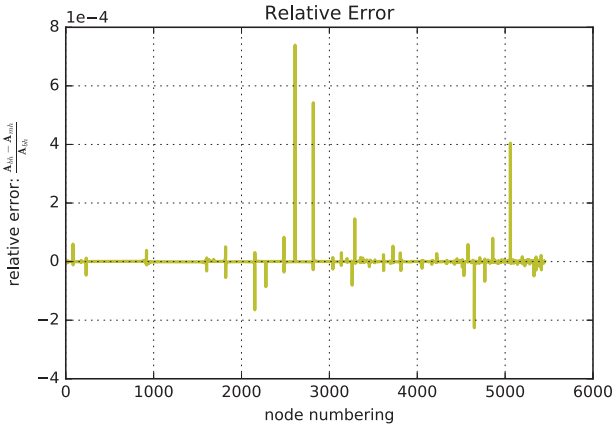

(b) Example of a rotating machine.

Fig. 13. Convergence plots

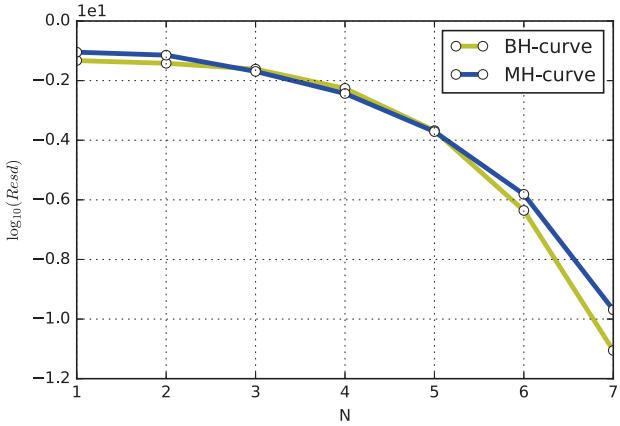

(a) Example of a linear machine.

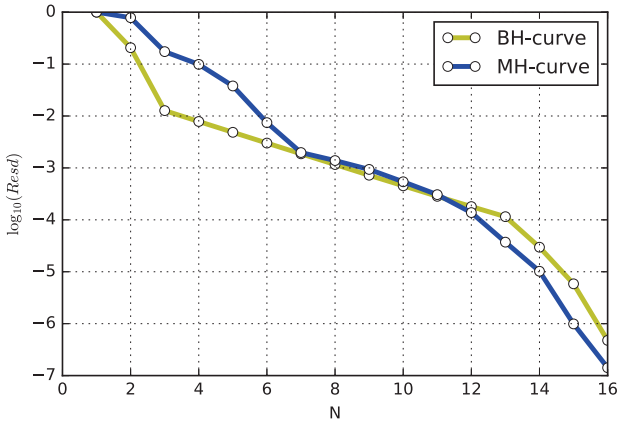

(b) Example of a rotating machine.

Fig. 14. Logarithm of the residuals against the number of iterations

[5] M.T. Darvishi and N. Darvishi . SOR- Steffensen-Newton Method to solve systems of nonlinear equations, Journal of Applied Mathematics 2012, 2(2): 21-27

[6] D.K.R. Babajee, M.Z. Dauhoo. An analysis of the properties of the variants of Newton's method with third order convergence, Appl. Math. Comput. 183, 659-684, 2006

[7] M.A. Hernandez. Second-derivative-free variant of the Chebyshev method for nonlinear equations, J. Opt. Theo. Appl. 104, 501-515, 2000.

[8] A. Cardero, J.R. Torregrosa. Variants of Newton's method for functions of several variables, Appl. Math. Comput, 183, 199-208, 2006.

[9] J.M. Ortega, W.C. Rheinboldt. Iterative solution of nonlinear equations in several variables, Academic Press, 1970.

[10] S. Yan, J-M Jin. Theoretical formulation of a time-domain finite element method for nonlinear magnetic problems in three dimensions, *Progress In Electromagnetics Research*, Vol. 153, 33-55, 2015.

[11] H.A. Haus, J.R. Melcher. Electromagnetic fields and energy, *Prentice Hall, Inc.*, 1989

[12] R.G. Harrison. Modeling high-order ferromagnetic hysteretic minor loops and spirals using a generalized positive-feedback theory, *IEEE Transactions on Magnetics*, Vol. 48 No. 3, pp. 1115-1129, March 2012.

[13] R.G. Harrison. Positive-feedback theory of hysteretic recoil loops in hard ferromagnetic materials, *IEEE Trans on Magnetics*, Vol. 47, No. 1, January 2011.

[14] E. Dlala. Comparison of models for estimating magnetic core losses in electrical machines using the finite-element method, *IEEE Trans on Magnetics*, Vol. 45, No. 2, February 2009.

[15] N.H. Kim. Introduction to Nonlinear Finite Element Analysis, Springer-Link : Bücher, *Springer US*, 2014.

[16] R. Bargallo. Finite elements for electrical engineering, *Electrical engineering department*, 2006.

[17] A. Chama. Study and Implementation of Two-dimensional Moving Finite Elements Method, MSc Thesis, University of KwaZulu-Natal, 2009.